TWENTY-FOURTH EUROPEAN ROTORCRAFT FORUM
Marseille, France, 15th-17th September 1998

Vibration and Noise Reduction through Individual Blade Control Experimental and Theoretical Results

Référence : TE10

D. Morbitzer
U.T.P. Arnold
M. Müller

ZF Luftfahrttechnik GmbH, Germany

1 Abstract

The paper reviews the current research activities at ZF Luftfahrttechnik (ZFL) in two very promising application areas of IBC: noise and vibration reduction. The former aim was subject of a recent flight test campaign whereas the latter one has primarily been treated by theoretical investigations.

The first chapter gives an overview of the IBC hardware set-up on board the helicopter, the test matrix, and the flight test procedure. Helicopter vibration and ground noise measurement results are presented and compared to corresponding wind tunnel data.

The second part reports some results of theoretical investigations on vibration reduction. Firstly, the influence of rotor blade properties (as number of blades, hinge offset and LOCK number, e.g.) on the predicted IBC effectiveness has been investigated using the rotor analysis code CAMRAD/JA. Additionally, the variation of IBC effectiveness versus flight speed has been examined.

The well-known quasi-steady vibration response matrix method is used to evaluate the feasibility of a straightforward gain scheduled open-loop control architecture. Finally, two different closed-loop control structures are investigated with regard to their transient behavior and convergence.

2 Notation

A_n	HHC control amplitude of n/rev harmonic component
a/R	relative (flap and lag) hinge offset
E	Higher harmonic control effectiveness with respect to vibrations
h	vertical distance rotor hub to c.g.
I_β	flapwise moment of inertia about hinge
L, M	rotor hub roll, pitch moment
N	number of blades
n	order of harmonic component
R	rotor radius
T	rotor thrust
$\underline{T}$	steady-state vibration response transfer matrix, see eq. (2)
$\underline{Z}$	vector of vibration harmonics
α_{Ro}	rotor angle of attack (with respect to plane perpendicular to shaft)
$\gamma = \frac{\rho c C_{l\alpha} R^4}{I_\beta}$	blade LOCK number
ϑ	blade pitch control angle
$\mu \approx \frac{V}{\Omega R}$	advance ratio
φ_n	HHC control phase angle of n/rev harmonic component, see eq. (1)
$\sigma = \frac{Nc}{\pi R}$	blade solidity
Ω	rotor rotational frequency

3 Introduction

Research activities over a period of almost 50 years have established the notion that the extension of the conventional 1/rev blade pitch control towards higher harmonic control should yield substantial benefits in multiple aspects of the rotor performance, refs. [1,2,3,4,5]. Although most of the studies have demonstrated considerable improvements with respect to rotor induced vibrations, BVI noise radiation, blade and pitch link loads, blade motion stability, power required, and high speed rotor limitations, neither Higher Harmonic Control (HHC) nor Individual Blade Control (IBC) have been implemented in a production rotorcraft and become operational so far.

Therefore, ZFL has pursued the development of hardware components which enable the introduction of genuine IBC to conventional swashplate controlled rotors. Having participated in several national and international research programs, ZFL

has become the primary designer and manufacturer of complete IBC systems, ref. [6].

Beside this role as IBC hardware designer and manufacturer, ZFL has gathered a broad spectrum of theoretical know-how that helps to explore the potential of IBC. Based on a solid data basis accumulated during various test campaigns, numerical simulation is used to predict the possible benefits of IBC and to investigate possible control system layouts, ref. [7].

4 Noise Reduction Flight Tests with BO-105 Helicopter

As mentioned above, ZFL has accumulated many hours in flight and wind tunnel testing of complete IBC systems. Building upon the experience gained during a 1990/1991 flight test campaign, ref. [8], ZFL is currently participating in the *Rotor Active Control Technology (RACT)* research program including two flight test campaigns. ZFL's partners in this program are Eurocopter Deutschland, DLR Braunschweig, University of Braunschweig, and Daimler Benz Forschung.

Due to the genuine IBC capability of the implemented ZFL hardware, control inputs are not restricted to discrete higher harmonic frequencies applied to all blades similarly. The full potential of IBC will be exploited by introducing a new time domain control architecture for the upcoming continuation of the flight tests.

The IBC system and a multitude of highly sophisticated data acquisition, transmission, and recording systems had been installed on a Eurocopter BO-105 helicopter, see Fig. 1. Basic flight test instrumentation was provided by Eurocopter whereas the high bandwidth rotor data acquisition system was designed and implemented by the DLR. The ground based noise measurement hardware (compliant with the ICAO regulations) supplemented the on board data acquisition, ref. [9].

The experimental IBC system is an enhanced version of the ZFL-built hardware which was already used during an earlier flight test campaign. The upgraded IBC actuators now allow for maximum amplitudes of ±1.1deg at a bandwidth of approximately 60Hz (corresponding to 8/rev). They are installed in the rotating frame between the swashplate and the pitch horn and replace the conventional rigid pitch rods. Actuator position, velocity, and axial force are continuously monitored for control and safety purposes. A fast mechanical locking mechanism provides fail-safe behavior in case of an unforeseen malfunction.

4.1 Prior Wind Tunnel Test Results

During a collaborative 1993/94 wind tunnel test campaign at NASA Ames, a slightly different ZFL-built IBC System was integrated in the control system of a full-scale BO-105 hingeless rotor. During two wind tunnel entries in the 40x80ft² test section, this set-up was used to investigate the effect of HHC (using 2/rev through 6/rev inputs) on rotor vibrations, noise, performance and blade structural loads.

For noise measurements, the rotor operating condition was adjusted to represent high BVI conditions as usually encountered during landing approaches. A sum of seven microphones at different lateral and axial locations on the advancing and retreating side of the rotor was used to measure the radiated noise. For a detailed description of the wind tunnel test hardware set-up see ref. [10].

The effect of HHC on rotor noise for a descent flight condition at $\mu = 0.15$ and a rotor angle of attack of 2.9deg corresponding to a flight path of γ = -6deg was extensively investigated. Different higher harmonic control inputs (single and mixed mode) according to

$$\vartheta_i(\psi_i) = \vartheta_0 + \ldots + \sum_{n=2}^{6} A_n \cos(n\,\psi_i - \varphi_n) \qquad (1)$$

as the pitch angle of the i-th blade have been investigated. It was found that a 2/rev HHC input had considerable effect on rotor noise. Fig. 2 shows the measured band-limited sound pressure levels as a function of the 2/rev control phase angle φ_2. The optimum phase was found at approx. 90deg with a reduction of more than 6dB on both rotor sides. The measured 4/rev vibratory hub loads for this test case are presented in Fig. 3. The rotor hub loads are converted into equivalent accelerations. At the optimum control phase angle for minimum noise the vibratory loads remain almost unchanged compared to the reference case without HHC.

Similar results are obtained for a 3/rev single harmonic control input. The optimum phase angle for minimum noise can be identified at $\varphi_3 \approx 150$deg, see Fig. 4. The achieved noise reduction at this phase angle is about 5dB with little effect on vibratory loads, see Fig. 5. The noise reduction on the retreating side for arbitrary phase angles supposedly result from the restricted number of microphone locations leading to insufficient observation of the entire sound pattern. Extensive analysis of the acquired noise data is given in ref. [11].

4.2 Test Matrix and Flight Procedure

One driving force to pick up the IBC flight tests was to validate the promising full-scale wind tun-

nel test results in the field of BVI noise radiation. The question to be answered was, whether those impressive results could be confirmed under realistic free flight conditions. Major differences compared to the wind tunnel set-up were the presence of other noticeable noise sources (as tail rotor and engines) and the different arrangement of the (ground) microphones.

During the careful re-evaluation of the wind tunnel noise data, the most promising control settings had been identified and were then used to set up the flight test matrix, see Fig. 6. Each test point was validated by at least one additional flight with the same HHC setting. On-line monitoring of the acquired noise data was done to improve measurement accuracy.

4.3 Flight Test Results

During the whole flight test campaign a large amount of data was acquired. Detailed data evaluation revealed considerable variation of flight condition parameters for several test points. Some measurements have been taken at unsteady flight conditions and have been neglected for further analysis to assure data reliability. A comparison of measured and demanded flight condition parameters is given in Fig. 7. Nevertheless, a large amount of suitable test data was collected providing a sufficient data base for current and future analysis.

Fig. 8 shows the maximum A-weighted sound pressure level L_{Amax} versus the single harmonic 2/rev blade pitch control phase angle φ_2. A maximum noise reduction of more than 5dB was achieved at $\varphi_2 \approx 60$deg near the expected optimum phase angle according to wind tunnel results. However, both advancing and retreating side noise levels show different behavior when comparing both wind tunnel and flight test, see Fig. 2. This is likely to be caused by different flight and trim conditions, the different microphone geometry as well as from the different noise radiation and reverberation for the wind tunnel configuration, ref. [11].

As can be seen in Fig. 9 a HHC input with the same phase angle almost entirely cancels 4/rev vibrations at the main gearbox as well as at the co-pilot seat. This result contrasts with former HHC results where noise and vibration reduction were never achieved simultaneously when using 3/rev, 4/rev and 5/rev swashplate higher harmonic control, ref. [12].

The effect of 3/rev on noise and vibrations are illustrated in Fig. 10 and Fig. 11, respectively. In general, the maximum noise reduction is smaller than that for 2/rev inputs. At phase angles of $\varphi_3 \approx 180$deg all microphones show reduced sound pressure levels. The deviation of the BVI noise response to HHC inputs between the advancing and retreating side is even more pronounced than for 2/rev control inputs. This suggests that the noise directivity is affected in the first place rather than the over-all noise effectively reduced. The physical effects, however, that cause the described discrepancies are still not fully understood and thus subject to further investigations.

Regarding helicopter vibrations, it was found that the applied HHC amplitude of 0.5deg was too large. To show the possible vibration reduction through 3/rev HHC, the calculated vibrations for the optimum control amplitude $A_{3,opt} = 0.37$deg for minimum gearbox and co-pilot seat accelerations are added to Fig. 12. Vibration reductions of approx. 70% for all components have been calculated. The fact that the gearbox and co-pilot seat vibration response correlates in terms of optimum control phase and amplitude, implies that the measured helicopter vibrations are fairly insensitive to sensor locations in the case of the BO-105.

5 Theoretical Investigation of Vibration Reduction Potential

Besides rotor noise, the reduction of helicopter vibrations through HHC/IBC has successfully been demonstrated in several experimental programs, ranging from MACH-scaled or full-scale wind tunnel tests to several flight test campaigns, refs. [4,13,14,15]. The spectrum of helicopter types covered by these experiments, however, is still far too narrow to yield reliable predictions for arbitrary rotorcraft. Consequently, theoretical investigations have been started at ZFL to improve prediction methods of the required actuation speed for different helicopters. The maximum actuation speed (and less predominantly control amplitudes) are driving the hardware requirements of an IBC system and thus decide upon system weight and cost.

5.1 Parameter Study on HHC Effectiveness

It is obvious that the transfer of IBC results from one type of rotor to another is subject to certain restrictions. The effects of higher harmonic blade pitch control strongly depend not only on the actual operating condition but also on the dynamic and aerodynamic properties of the rotor.

Definition of IBC effectiveness All investigations presented herein base on the quasi-steady frequency domain model for helicopter vibrations. This model relates the cosine and sine harmonics of higher harmonic pitch control angle $\underline{\vartheta}$ to the produced

helicopter vibrations $\Delta\underline{Z}$, usually measured in the non-rotating frame, and can be written as

$$\underline{Z} = \underline{\underline{T}}\,\underline{\vartheta}_{HHC} + \underline{Z}_0 \quad , \; \underline{Z}_0 : \text{ref. vibrations} \qquad (2)$$

Such a HHC model is appropriate for linear time-periodic (LTP) systems, ref. [16]. If only single harmonic control is applied, the T-matrix describes an ellipse in the sine/cosine plane of each vibratory component as shown in Fig. 12. The shape and size of each ellipse depend on the T-matrix components. The effectiveness of higher harmonic control may be defined as the ratio of produced vibration $\Delta\underline{Z}$ to HHC input, i.e. $|\Delta\underline{Z}|/|\underline{\vartheta}_{HHC}|$. The mean vibratory response can be approximated by the radius E of a circle having the same area as the actual ellipse. This definition is applied to all HHC input and vibration harmonics. The over-all HHC effectiveness can then be written as

$$E = \frac{1}{qp}\sum_{j=1}^{q}\sum_{i=1}^{p} E_{ji} \qquad (3)$$

for q vibratory loads and p HHC input frequencies. In the following chapters, the influence on N/rev harmonics of longitudinal, lateral and vertical hub forces as well as rotor pitch and roll moments are concerned. To avoid dimensional inconsistencies the moments are divided by the vertical distance h from the rotor hub to the aircraft's over-all center of gravity.

Influence of LOCK number and hinge offset The potential of vibration reduction through HHC results from the ability to change aerodynamic and inertial loads acting on each rotor blade. Two important rotor parameters in this connection are the LOCK number γ describing the ratio of aerodynamic to inertial forces and the relative hinge offset a/R. The latter strongly affects the blade eigenfrequencies and hence the dynamic properties of the rotor.

Using the rotor analysis code CAMRAD/JA a systematic variation of both parameters was carried out. For each a/R–γ configuration the response of the N/rev vibratory hub loads to HHC was calculated for different HHC phase angles yielding the transfer matrix $\underline{\underline{T}}$ and thus the effectiveness E. The LOCK number was varied by changing the constant mass distribution. Note that γ slightly changes for varying hinge offset a/R due to the decreasing moment of inertia I_β about the hinge. Relevant CAMRAD/JA model parameters are summarized in Tab. 1.

For this 4-bladed rotor with perfectly equal blades the 4/rev hub loads in the non-rotating frame only result from 3/rev, 4/rev and 5/rev vibratory loads in the rotating frame. Significant but not exclusive contributions to these blade load harmonics are made by HHC with the corresponding frequencies. Therefore, the present study concentrates on the effectiveness of these HHC frequencies.

Fig. 13 through Fig. 15 show the results of this parameter study for 3/rev, 4/rev, and 5/rev HHC inputs. Additionally, parameter combinations that correspond to existing helicopters are marked in the figures to illustrate existing design configurations.

The contours of constant HHC effectiveness are quite different for the three input harmonics. The 4/rev effect is almost insensitive to the LOCK number γ. Significant high effects can be realized at large hinge offsets whereas much lower effectiveness is present at $a/R = 0.04$. This effectiveness „notch" mostly results from a reduced effect on the rotor thrust which contributes to a large amount to the over-all effectiveness as defined in eq. (3).

Highest 3/rev effects are obtained at large hinge offsets and LOCK numbers, i.e. light weight blades. A remarkable result is that E stays almost the same for such different rotor types as the BO-105 and the CH-53. Since the simulations are based on four bladed rotors, this result, however, should not directly be transferred to the actual CH-53G helicopter with six rotor blades. The influence of the blade number N will be presented later. Finally, the 5/rev HHC effectiveness is somewhat smaller for all a/R–γ configurations. A rather large area of reduced effectiveness can be found near $\gamma = 9$ and $a/R = 0.08$.

Influence of forward speed An implemented vibration controller must cover the whole flight envelope. Since the rotor encounters strong changes of its aerodynamic operating condition, the potential of HHC to produce anti-vibratory loads is expected to change with forward speed, too. To estimate the required control authorities the extent to which the HHC effectiveness varies for different flight conditions has to be known. Further investigations of flight speed sensitivity of HHC required identification accuracy for open-loop control will be discussed later.

Fig. 16 summarizes the CAMRAD/JA results based

Rotor	wind tunnel configuration
number of blades	$N = 4$
hub configuration	articulated
radius	$R = 4.9$m
DOF's	2 flapwise, 1 lead-lag and 1 torsional mode
Aerodynamics*	
inflow model	free-wake
advance ratio	$\mu = 0.1$
blade loading	$C_T/\sigma = 0.07$

*) aerodynamic properties similar to BO-105 rotor.

Table 1: CAMRAD/JA model parameters for a/R-γ parameter study.

on a detailed BO-105 model (see Tab. 2) for the effectiveness of 3/rev, 4/rev and 5/rev as a function of the advance ratio μ. Although there is no dramatic change at specific flight speeds, it must be noted that E does not generally increase with speed. Similarly, wind tunnel results indicate that the HHC effectiveness remains almost constant. For high speed conditions usually high levels of vibrations are encountered, thus the required HHC authorities to cancel the higher vibrations are expected to increase with forward speed, too.

Influence of Blade Number Considering the application of IBC on a broad spectrum of helicopters the question arises if the blade number has influence on the effectiveness. A CAMRAD/JA parameter study has been carried out using the same detailed model of the BO-105 as the baseline data set, see Tab. 2.

The blade number has been varied, with blade chord set to corresponding values to maintain constant blade loading C_T/σ for constant aircraft mass. All other blade properties and thus dynamics were held constant which is more or less correct for existing rotor configurations with different number of blades, e.g. Sikorsky's CH-53 and its derivatives.

Rather than focusing on the over-all HHC effectiveness, the rotor hub forces and moments are examined separately. Whereas the rotor thrust is basically the sum of all vertical blade shear forces the rotor roll and pitch moments are determined by expressions like

$$L = \sum_{i=1}^{N} M_{\text{flap},i} \sin\psi_i \qquad (4)$$

$$M = \sum_{i=1}^{N} M_{\text{flap},i} \cos\psi_i \qquad (5)$$

Due to the cosine and sine modulation of the root flapwise bending moments M_{flap}, contribution to the N/rev harmonics of L and M are only made by harmonics of frequency (N-1)/rev and (N+1)/rev. This contrasts with the direct transmission of N/rev vertical shear forces to N/rev rotor thrust.

Fig. 17 (a) shows the HHC influence on the N/rev rotor thrust as a function of blade number and HHC frequency. Note that not only (N-1)/rev, N/rev, and (N+1)/rev HHC have been analyzed. The shaded bars indicate the N/rev HHC cases resembling a ridge along the diagonal line of corresponding blade number and HHC frequency. The largest effect on vibratory vertical hub loads is found for the 5-bladed rotor. A remarkable contribution from 4/rev has been found for all blade numbers. It even exceeds the 3/rev effectiveness for the 3-bladed rotor. Furthermore also 2/rev inputs affect the N/rev vertical force to some extent, especially for the 5-bladed rotor.

HHC impact on the N/rev pitch and roll moments are presented in Fig. 17 (b). The (N-1)/rev and (N+1)/rev harmonic inputs, which have the largest effect on hub moments, are shown as shaded bars. Due to the transformation from the rotating to the non-rotating frame, see eqs. (4,5), the ridge is expected to split into two parts. However, 4/rev HHC considerably affects the hub moments for all blade number configurations.

Rotor	horizontal free flight
hub configuration	hingeless
radius	R = 4.9m
DOF's	5 flapwise, 5 lead-lag bending modes (coupled), and 3 torsional modes
Aerodynamics	
inflow model	free-wake

Table 2: CAMRAD/JA model parameters for flight speed variation and blade number parameter study.

5.2 Potential of Vibration Reduction by Open-Loop Control

Most investigations on vibration reduction through HHC/IBC are based on the a priori assumption that an efficient control system has to be of closed-loop structure. However, it is difficult to find published data that prove the assumption, that the optimum higher harmonic control settings are sensitive to certain flight condition parameters and therefore the application of closed-loop control is inevitable.

Considering cost and complexity it would surely be attractive to base a straight forward controller on a gain scheduled open-loop structure. The generation of suitable, though suboptimal control inputs would simply rely on stored data describing the relation between the flight condition and optimum higher harmonic control inputs.

Building again on the well-known T-matrix approach as the underlying model, see eq. (2), it was investigated how much control fidelity has to be sacrificed if open-loop control is used.

The flight speed is expected to be an important parameter that affects the helicopter's reference vibration $\underline{Z}_0$ as well as the transfer matrix $\underline{\underline{T}}$, primarily with respect to phase shift of the vibration response. Hence, a specific optimum input vector $\underline{\vartheta}_{\text{HHC}}$ exists for a given flight speed. For an equal number of measured vibratory components and HHC inputs, the optimum control can be determined by

$$\underline{\vartheta}_{\text{opt}} = -\underline{\underline{T}}^{-1}\underline{Z}_0 . \qquad (6)$$

Since $\underline{\vartheta}_{\text{opt}}$ is a function of flight speed, i.e. advance ratio, the correct input is only chosen by the controller if μ is perfectly known. In general, meas-

urement errors $\Delta\mu$ are always present and the wrong inputs scheduled for $\mu_{meas} = \mu_{real} + \Delta\mu$ are generated instead leading to residual vibrations $\underline{Z}_{res}$. Fig. 18 depicts the described open-loop control scheme.

The residual vibrations at a given advance ratio depend on the sensitivities of the T-matrix and the reference vibrations to the incorrectly measured speed. Based on CAMRAD/JA simulations for the BO-105 helicopter, this effect was evaluated over forward speed. For a given maximum measurement error $\Delta\mu$ the residual vibrations can be determined by

$$\underline{Z}_{res}(\mu) = \underline{\underline{T}}(\mu) \cdot \underline{\vartheta}_{HHC}(\mu + \Delta\mu) + \underline{Z}_0(\mu) . \quad (7)$$

Fig. 19 shows the remaining vibrations (averaged from the three separate control paths 3/rev → L/h, 4/rev → T, and 5/rev → M/h) versus the advance ratio for a constant measurement inaccuracy of 3m/s as well as for a relative flight speed error of 5%. The residual vibrations are particularly high at low and high speed conditions were usually high levels of helicopter vibrations are encountered. Very similar results have been obtained using T-matrices and reference vibrations from wind tunnel test data.

Since an open-loop controller has to adapt to other flight condition parameters as well, e.g. vertical speed, rotor thrust etc., the controller's performance in reducing vibrations is likely to be worse than in the presented case. However, it will depend on the availability of highly accurate flight condition measurements, whether open-loop control can assure acceptable vibration reduction performance.

5.3 Assessment of Different Closed-Loop Controller Variants

Closed-loop vibration control on one hand offers better vibration reduction performance than gain-scheduled open-loop control, but will increase system complexity and can introduce dynamic stability problems on the other hand.

A fundamental question when considering IBC for vibration reduction is, how the knowledge of the plant to be controlled can be incorporated into a suitable (closed-loop) control structure. Several approaches of closed-loop vibration control of either frequency or time domain controller schemes have been reported in the literature, refs. [3,14,15]. An excellent overview of frequency domain HHC algorithms is given by Johnson, ref. [17]. The basic idea behind these schemes is to calculate HHC inputs by applying the inverse T-matrix to the measured N/rev vibration harmonics.

The control law to determine the control input at time step k can be written as

$$\underline{\vartheta}_k = \underline{\vartheta}_{k-1} - \underline{\underline{T}}^{-1}\, \underline{Z}_{k-1} . \quad (8)$$

Note that in case of unequal number of vibratory loads and HHC inputs $\underline{\underline{T}}$ is not a square matrix thus $\underline{\underline{T}}^{-1}$ does not exist. In that case a modified feedback matrix, in general referred to as the controller gain matrix $\underline{\underline{H}}$, must be used.

If $\underline{\underline{T}}$ is perfectly known and the quasi-steady model is valid eq. (8) leads to dead-beat control in a single controller step. However, modeling errors are always present thus multiple steps are necessary for complete vibration rejection. Regarding variation of the T-matrix, Johnson focused on identification methods that secure closed-loop performance and stability. Despite that, it was found that even a fixed-gain controller with optimized feedback matrix $\underline{\underline{H}}$ was robust and performed satisfactory for all investigated flight conditions, ref. [18].

Usually, one or more rotor revolutions are required to calculate the vibration harmonics by FFT. Thus, the HHC inputs are updated at discrete time steps. Fig. 20 (a) depicts the block diagram of such a discrete time frequency domain vibration controller. The integrating character of the control law, see eq. (8), leads to perfect vibration rejection even if the gain matrix $\underline{\underline{H}}$ includes modeling errors. In fact, $\underline{\underline{H}}$ should be chosen only as a fraction of $-\underline{\underline{T}}^{-1}$ to limit the HHC input rates.

A continuous-time harmonic decomposition was suggested by Hall, ref. [16]. By modulating the measured vibration time signals with harmonic functions with a frequency of N/rev, the required vibration harmonics can be extracted. The controller is then updated continuously without waiting for the next FFT results. The corresponding controller block diagram is presented in Fig. 20 (b).

To assess the two variants' performance, a linear state-space model for the vibratory loads in the-rotating frame as functions of blade pitch input was extracted from CAMRAD/JA and implemented for each rotor blade. The actuators' dynamics have also been included through a benchtest validated transfer function model. Three vibratory loads and (N-1)/rev, N/rev, and (N+1)/rev control have been considered yielding a 6x6 square gain matrix.

Simulation results for both the discrete-time and continuous-time controller scheme are shown in Fig. 21. The latter shows faster vibration rejection without input overshoots. Consequently, the continuous time variant is likely to provide better performance for disturbed vibrations as well as for changing rotor dynamics due to different flight conditions.

6 Conclusions

During the past few years ZFL has gathered a broad spectrum of IBC related data originating from flight and wind tunnel tests as well as from theoretical investigations. The potential of IBC to reduce helicopter noise and vibrations has been lately proven in an extensive flight test campaign. Remarkable levels of reductions were achieved for noise and vibrations simultaneously.

Through detailed theoretical investigations and parameter studies of the HHC effectiveness with respect to vibratory hub loads the ability to predict IBC design parameters, i.e. required blade pitch authorities and actuation speed, has been improved. However, detailed prediction of active rotor control effects must be based on detailed rotor data.

It was found that for an open-loop control scheme with gain-scheduled HHC inputs, the speed measurement accuracy is crucial for the controller's vibration reduction potential. This may cause some difficulties particularly at low forward speed. Additionally, two different closed-loop control structures, both formulated in the frequency domain, have been analyzed. Whereas both variants offer the same potential reduction levels, the continuous-time implementation tends to show better transient performance.

7 References

[1] E.R. Wood, R.W. Powers, J.H. Cline, C.E. Hammond, **On Developing and Flight Testing a Higher Harmonic Control System,** 39th AHS Annual Forum, St. Louis, 1983.

[2] G. Reichert, **Helicopter Vibration Control - A Survey,** 6th European Rotorcraft Forum, Bristol, 1980.

[3] C.E. Hammond, **Wind Tunnel Results Showing Rotor Vibratory Loads Reduction Using Higher Harmonic Blade Pitch,** 36th AHS Annual Forum, Washington D.C., 1980.

[4] M. Polychroniadis, M. Achache, **Higher Harmonic Control: Flight Tests of an Experimental System on SA 349 Research Gazelle,** 42nd AHS Annual Forum, Washington D.C., 1986.

[5] D. Teves, G. Niesl, A. Blaas, S. A. Jacklin, **The Role of Active Control in Future Rotorcraft,** 21st European Rotorcraft Forum, Saint-Petersburg, 1995.

[6] P. Richter, H.-D. Eisbrecher, V. Klöppel, **Design and First Tests of Individual Blade Control Actuators,** 16th European Rotorcraft Forum, 1990.

[7] U.T.P. Arnold, M. Müller, P. Richter, **Theoretical and Experimental Prediction of Individual Blade Control Benefits,** 23rd European Rotorcraft Forum, Dresden, 1997.

[8] D. Teves, V. Klöppel, P. Richter, **Development of Active Control Technology in the Rotating Frame, Flight Testing and Theoretical Investigations,** 18th European Rotorcraft Forum, Avignon, 1992.

[9] D. Schimke, U.T.P. Arnold, R. Kube, **Individual Blade Root Control Demonstration - Evaluation of Recent Flight Tests,** 54th AHS Annual Forum, Washington D.C., 1998.

[10] S. A. Jacklin, A. Blaas, S. M. Swanson, D. Teves, **Second Test of a Helicopter Individual Blade Control System in the NASA Ames 40- By 80-Foot Wind Tunnel,** 2nd AHS International Aeromechanics Specialists Conference, 1995.

[11] S.M. Swanson, S.A. Jacklin, A. Blaas, G. Niesl, R. Kube, **Acoustic Results from a Full-Scale Wind Tunnel Test Evaluating Individual Blade Control,** 51st AHS Annual Forum, Fort Worth, 1995.

[12] W. R. Splettstoesser et al., **BVI Impulsive Noise Reduction by Higher Harmonics Pitch Control: Results of a Scaled Model Rotor Experiment in the DNW,** 17th European Rotorcraft Forum, Berlin, 1991.

[13] J. Shaw, N. Albion, **Active Control of the Helicopter Rotor for Vibration Reduction,** Vertica, Vol. 4, pp. 3-11, 1980.

[14] G. Lehmann, **Investigations on Higher Harmonic Blade Pitch Control at Helicopters,** Ph.D. Thesis (in German), Institute of Flight Mechanics, Technical University Braunschweig, 1987.

[15] N.D. Ham, **Helicopter Individual Blade Control: Promising Technology for the Future Helicopter,** 21th European Rotorcraft Forum, Saint-Petersburg, 1995.

[16] S. Hall, N. M. Wereley, **Linear Control Issues in the Higher Harmonic Control of Helicopter Vibrations,** 45th AHS Annual Forum, Boston, 1989.

[17] W. Johnson, **Self-Tuning Regulators for Multicyclic Control of Helicopter Vibration,** NASA Technical Paper, 1982.

[18] R. Kube, **Effects of Blade Elasticity on Open- and Closed-Loop Higher Harmonic Control of a Hingeless Helicopter Rotor,** Ph.D. Thesis (in German), DLR research report FB 97-26, Braunschweig, 1997.

Figure 1: Experimental helicopter BO-105 S1 with high authority IBC system during flight test.

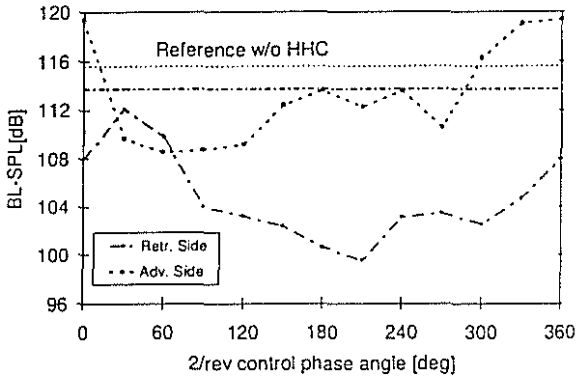

Figure 2: Band limited sound pressure level *vs.* phase angle for single harmonic 2/rev control with A_2 = 1.0deg (wind tunnel data, full-scale BO-105 rotor, μ = 0.15, α_{Ro} = 2.9deg).

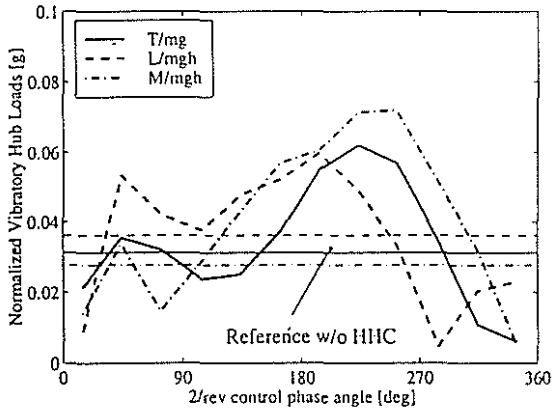

Figure 3: Vertical rotor hub vibrations *T/mg*, *L/mgh* and *M/mgh vs.* phase angle for single harmonic 2/rev control with A_2 = 1.0deg (wind tunnel data, full-scale BO-105 rotor, μ = 0.15, α_{Ro} = 2.9deg).

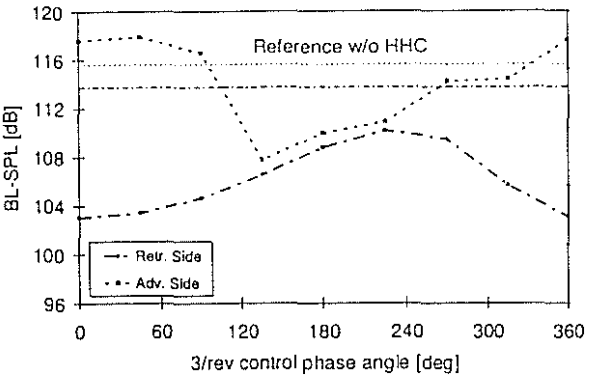

Figure 4: Band limited sound pressure level *vs.* phase angle for single harmonic 3/rev control with A_3 = 0.5deg (wind tunnel data, full-scale BO-105 rotor, μ = 0.15, α_{Ro} = 2.9deg).

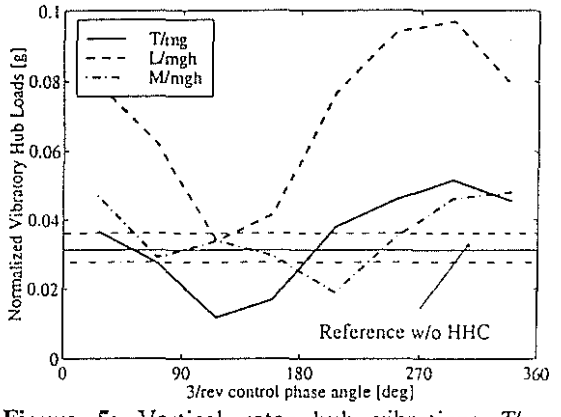

Figure 5: Vertical rotor hub vibrations *T/mg*, *L/mgh* and *M/mgh vs.* phase angle for single harmonic 3/rev control with A_3 = 0.5deg (wind tunnel data, full-scale BO-105 rotor, μ = 0.15, α_{Ro} = 2.9deg).

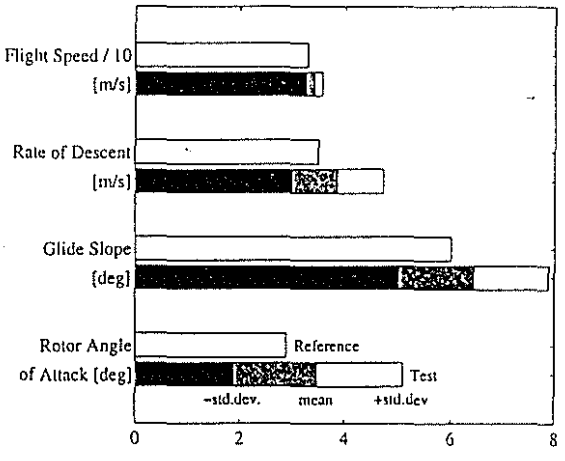

Figure 7: Comparison of demanded and measured flight condition data for landing approaches.

Run No.	Flight Condition	Indicated Air Speed V_{IAS} [kt]	Adv. Ratio μ [-]	Rate of Descent ROD [ft/min]	Glide Slope γ [°]	IBC-Mode n/rev [-]	IBC-Magnitude A_n [°]	IBC-Phase φ_n [°]
1	Landing approach with high BVI noise	65	0,15	692	-6	2	1.0	0 ... 330 $\Delta\varphi = 30°$
2						2	0.8	60
3						2	0.6	60
4						2	0.4	60
5						3	0.5	0, 90, 180, 270
6						3 5	0.5 1.0	210 30, 90 ,150
7	Determination of landing approach with highest BVI noise	65	0,15	460	-4	–	–	–
8				925	-8	–	–	–
9				1160	-10	–	–	–
10	Horizontal flight (500 ft) with optimum IBC input for min. vibrations	110 (V_h)	0,26	–	–	3	0.975	156
						4	0.645	356
						5	0.467	2
11						3	1.36	200
						4	0.79	96
						5	0.56	61
12						3	0.664	182
						4	0.152	42
						5	0.184	249

Figure 6: *Test matrix of IBC flight test.*

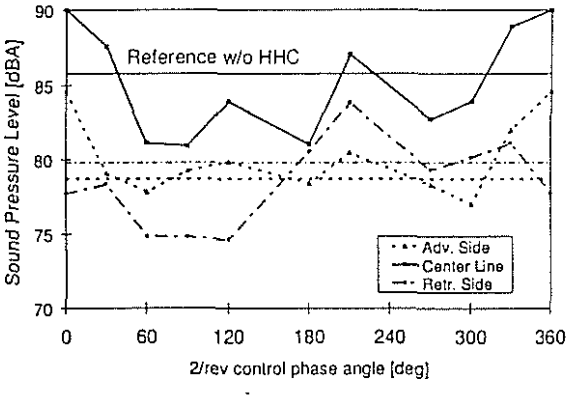

Figure 8: Rotor noise *vs.* phase angle for single harmonic 2/rev control with A_2 = 1.0deg (flight test data, *BO-105 S1*, $\mu = 0.15$, $\gamma = -6deg$).

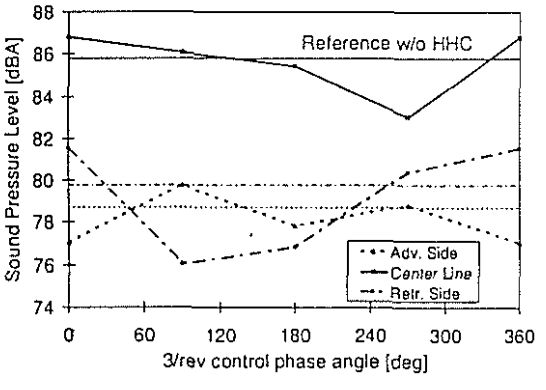

Figure 10: Rotor noise *vs.* phase angle for single harmonic 3/rev control with A_3 = 0.5deg (flight test data, BO-105 S1, $\mu = 0.15$, $\gamma = -6deg$).

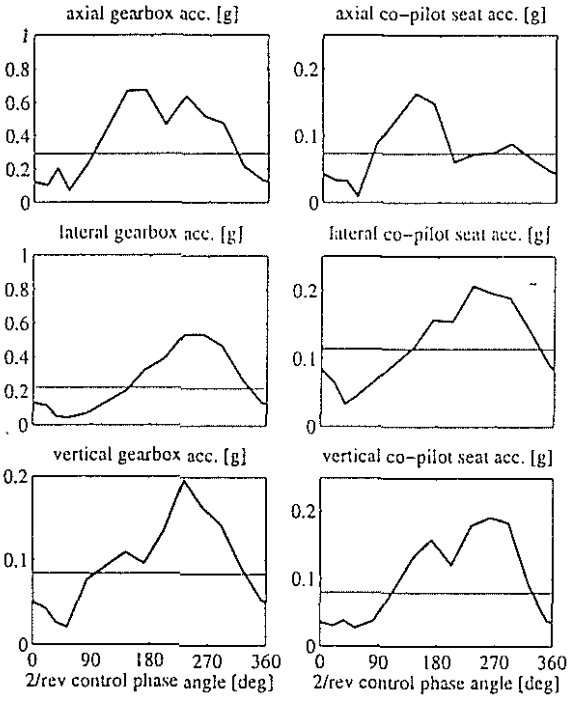

Figure 9: Accelerations at main gearbox and co-pilot seat *vs.* phase angle for single harmonic 2/rev control with A_2 = 1.0deg (flight test data, BO-105 S1, $\mu = 0.15$, $\gamma = -6deg$).

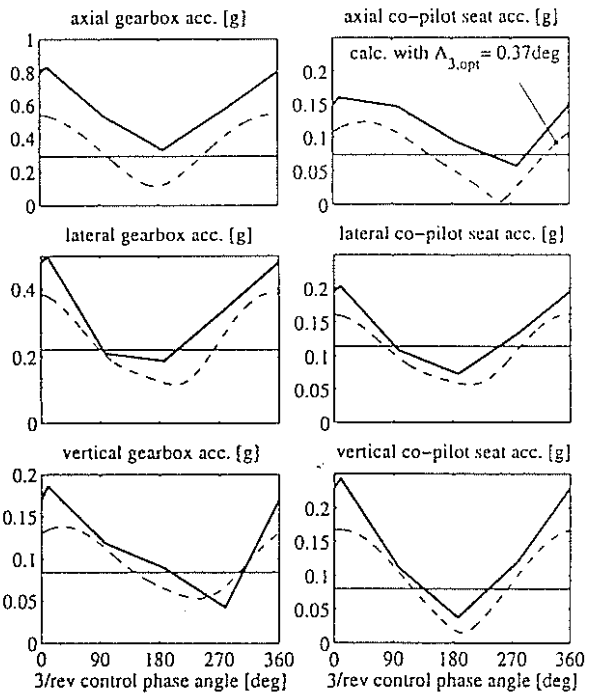

Figure 11: Accelerations at main gearbox and co-pilot seat *vs.* phase angle for single harmonic 3/rev control with $A_3 = 0.5$deg (flight test data, BO-105 S1, $\mu = 0.15$, $\gamma = -6$deg).

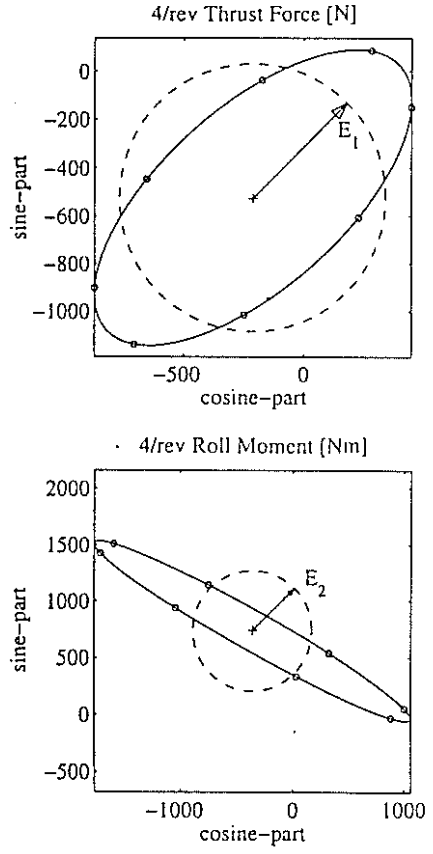

Figure 12: Definition of HHC effectiveness; this example: effect of 3/rev control input on 4/rev thrust force and roll moment response (wind tunnel data, full-scale BO-105 rotor, $\mu = 0.3$, $\alpha_{Ro} = -7.6$deg).

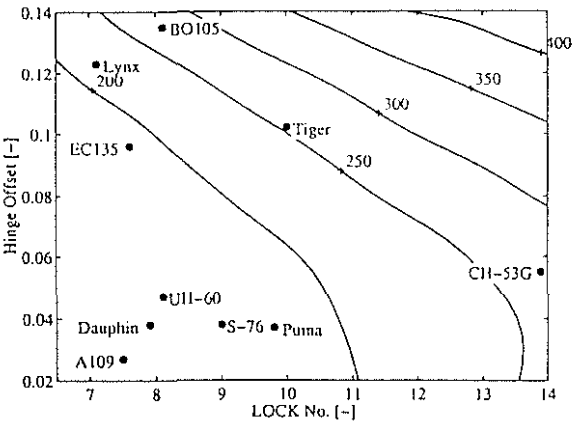

Figure 13: Influence of LOCK number and hinge offset on 3/rev HHC effectiveness (CAMRAD/JA results).

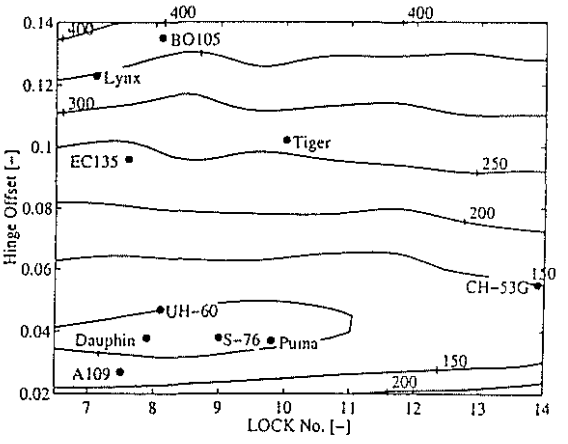

Figure 14: Influence of LOCK number and hinge offset on 4/rev HHC effectiveness (CAMRAD/JA results).

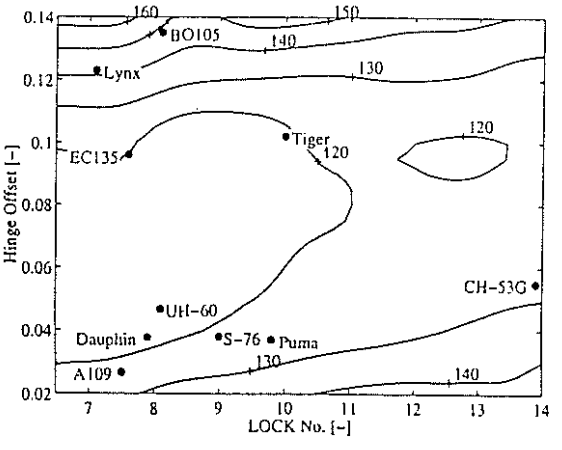

Figure 15: Influence of LOCK number and hinge offset on 5/rev HHC effectiveness (CAMRAD/JA results).

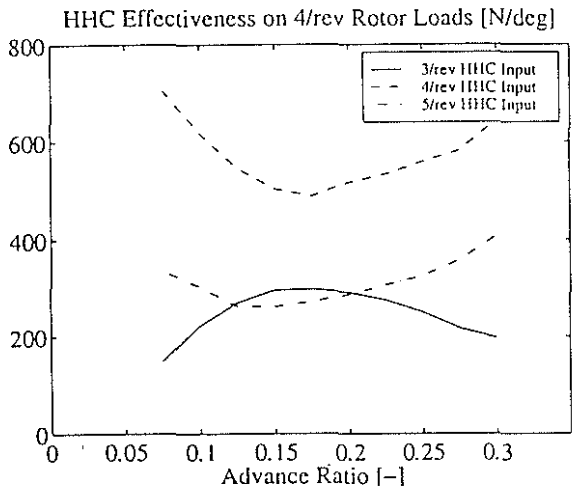

Figure 16: Effect of forward speed on HHC effectiveness for the BO-105 helicopter (CAMRAD/JA results).

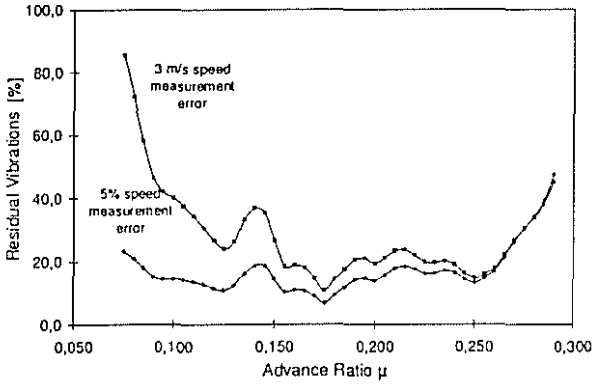

Figure 19: Residual vibrations *vs.* forward speed for given speed measurement error (T-matrix identified from CAMRAD/JA results).

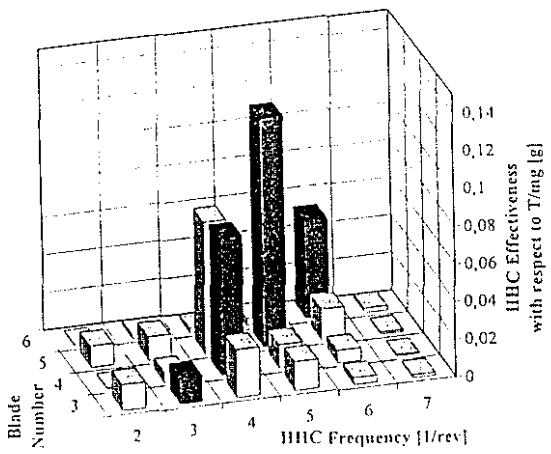

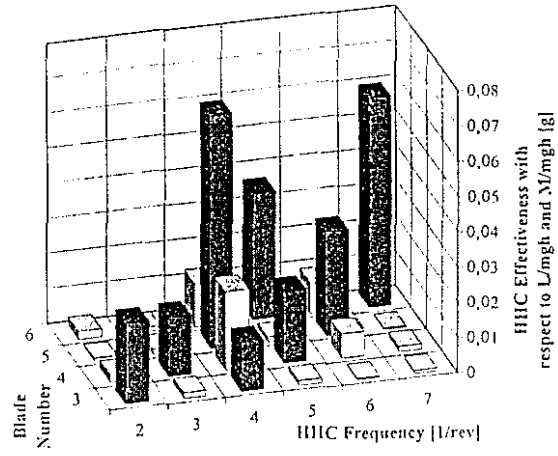

Figure 17: Effect of blade number on HHC effectiveness (CAMRAD/JA results based on BO-105 data set, C_T/σ = const.);
(a) Effectiveness on N/rev rotor thrust;
(b) Effectiveness on N/rev roll and pitch moment.

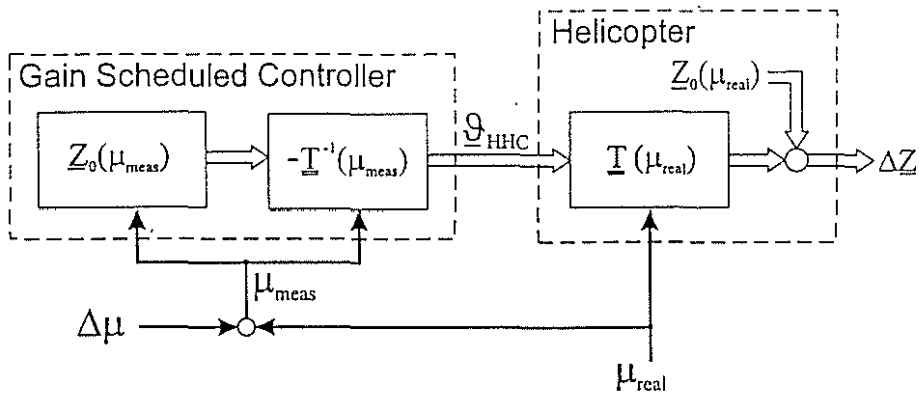

Figure 18: Vibration control structure used to investigate the effect of speed sensor inaccuracies on open-loop control fidelity.

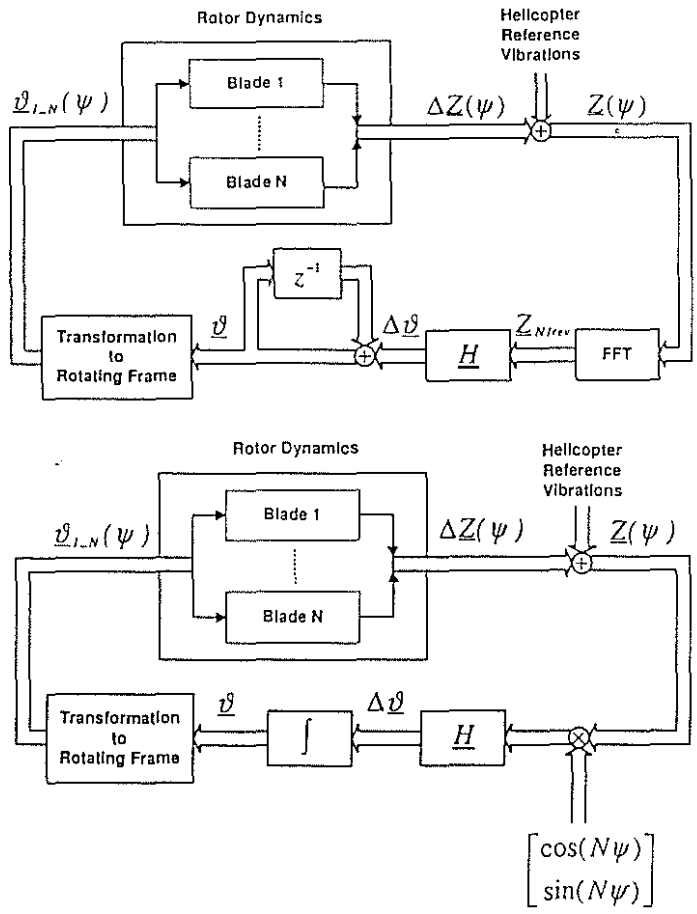

Figure 20: Block diagrams of two different closed-loop vibration control architectures;
(a) Discrete time implementation;
(b) Continuous time implementation.

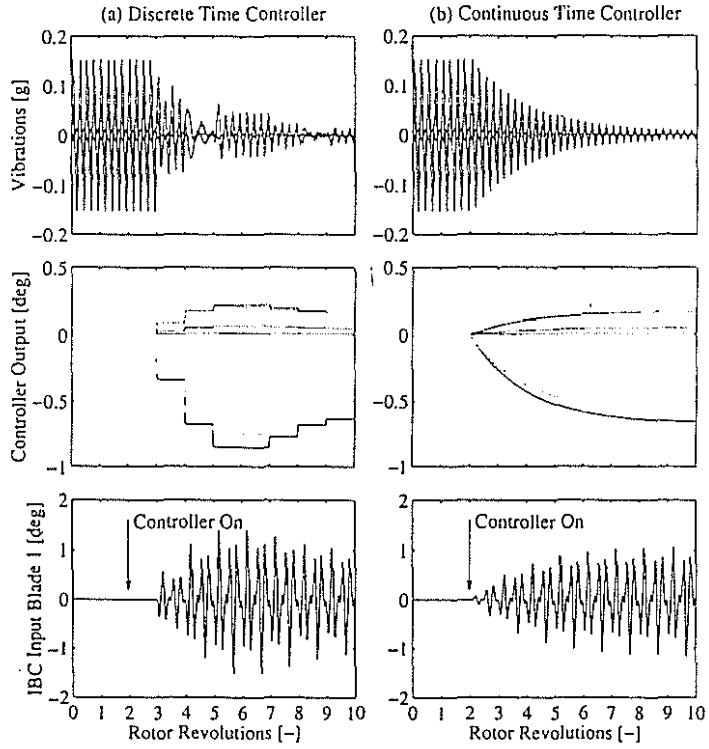

Figure 21: Simulated performance of two different vibration controllers (compare block diagrams in Fig. 20; discrete sample time for (a) set to T_S = 1rev).